ISSN 2319 - 6629
Volume 6, No.2, February – March 2017
International Journal of Wireless Communications and Networking Technologies
Available Online at http://warse.org/IJWCNT/static/pdf/file/ijwcnt03622017.pdf

Downlink Coverage Probability in Multi-Tier Rician Fading HetNets

Aditi Singh [1], Laurie L. Joiner [2], Adam Panagos [3]
[1]University of Alabama in Huntsville, Huntsville, AL, USA, as0086@uah.edu
[2]University of Alabama in Huntsville, Huntsville, AL, USA, joinerl@uah.edu
[3]Dynetics Inc., Huntsville, AL, USA, agp0002@uah.edu

ABSTRACT

Heterogeneous cellular networks (HetNets), consisting of macrocells overlaid with small cells, have become an integral part of existing cellular wireless networks to satisfy an ever increasing demand for mobile broadband applications and services. In this paper, the coverage probability in a downlink HetNet, comprising of multi-tier MIMO Base Stations (BSs) serving multiple users, assuming Rician-Rayleigh fading has been evaluated. Also, comparison of the Area Spectral Efficiency (ASE) for multi-user (MU) MIMO with the single-input single-output (SISO) case, demonstrates the gain in performance MIMO techniques can provide. Through simulation it has been demonstrated that as the number of users increase, the inter-stream interference increases, resulting in a reduction of coverage probability.

Key words: coverage probability, HetNets, MIMO, Rician fading

1. INTRODUCTION

Wireless communication systems using multiple- input multiple-output (MIMO) antennas have emerged as one of the most significant breakthroughs in modern communications [1]. Intensive research has been carried out in the field of MIMO systems since its advent in the late 1990s. These advances have caused MIMO systems to substantially increase data rate and reliability without consuming extra spectrum and resources. The advancement in technology adds new features and capabilities to the wireless networks, but it may leave some users uncovered and under-served. Small cells are used in such scenarios to provide coverage in remote locations and increase the data capacity in high demand congested urban areas.

To fulfill the demands of data hungry applications in high-traffic areas, the cellular systems are becoming denser and increasingly irregular. As a result, small cells are deployed opportunistically to fulfill the demands of users in densely populated areas. Thus, our current paradigm shift can be described based on the switch from carefully planned homogeneous networks to irregular deployment of Heterogeneous cellular networks (HetNets).

One of the key challenges in small cell deployment is its complexity in managing the numerous nodes in accordance with the different features they possess. The most commonly used simulation deployment models involve placing the base stations on a regular grid pattern, with mobile users either randomly or deterministically placed. However, the results obtained using the regular grid patterns are highly idealized and not very tractable [2]. Therefore, a common, tractable, and analytically convenient assumption for Base Stations (BSs) distribution in wireless networks is the homogeneous Poisson point process (PPP) of intensity λ. In this model, the number of nodes in a certain area of size A is Poisson distributed with parameter λA, and the numbers of nodes in two disjoint areas are independent random variables [3]. In the assumption of a PPP network, the BSs locations are modeled randomly according to the intensity of the PPP.

1.1 Related Work

Dhillon et. al have discussed the modeling and analysis of multi-tier downlink HetNets for single antenna BSs in a Rayleigh fading environment [4]. In a subsequent work, an upper bound has been derived for coverage probability in MIMO HetNets. Also, the modeling of downlink multi-antenna HetNets to determine coverage and Area Spectral Efficiency (ASE) in Rayleigh Fading has been discussed in [5]. Ordering results for coverage probability and per user rate have been derived to compare various transmission techniques in MIMO, such as Space Division Multiple Access (SDMA) and Single-user beamforming (SU-BF). Their performance analysis is explained in [6].

Hoydis et al. investigated ergodic mutual information and outage probability in small cell networks for Rician fading MIMO channels [7]. Also, the coverage probability from a macrocell users perspective has been analyzed assuming Rician fading in [8]. However, the analysis is restricted to a two tier network. The performance results in a Rician fading scenario are few in comparison to results for Rayleigh fading channel.

1.2 Motivation

The modeling of multi-antenna HetNets in Rayleigh fading with multiple classes of BSs, which have distinctly different traits, has been investigated in [5]. However, with densification of cells, the desired user often has a line-of-sight (LoS) to the receiver, in which case modeling the corresponding channel as Rician fading is more suitable. Although the coverage probability for macrocell users in Rician fading has been discussed in [8], small cells, which have become an integral part of the cellular networks with increasing demand of transmission rates and connectivity, have not been studied in conjunction with Rician fading. In

this paper, we determine the coverage probability and Area Spectral Efficiency for Rician-Rayleigh fading, i.e., the intended stream undergoes Rician fading, whereas the interfering streams undergo Rayleigh fading in multi-antenna, multi-tier HetNets. We use the approach from [4],[6] as the first step in our system design to model the positions of the BSs and mobile user. This research contributes the following new results:

- Analytical evaluation of coverage probability in Rician fading environment.
- Comparison of coverage probability in Rician and Rayleigh fading environment.
- Evaluation of area spectral efficiency (ASE) and the effect of Rician fading factor on ASE.

The organization of the paper is as follows:
Section 2 describes the system model and channel model used in obtaining the results for HetNets. In Sections 3 and 4, coverage probability and area spectral efficiency are defined, respectively, to understand the results obtained in the following section. Section 5 discusses the coverage probability and ASE results obtained by Monte Carlo simulation of HetNets in Rician Fading environment. Section 6 concludes and summarizes the results of this paper and presents ideas for future work.

2. SYSTEM MODEL

2.1 System setup and Channel Approach

We consider a multi-tier, multi-antenna heterogeneous cellular network with base station locations modeled as a two-dimensional spatial Poisson point process (PPP). The BSs across tiers differ in terms of their transmit power, the deployment density, target SIR and the multi-antenna technique employed [5]. All the tiers are in the same frequency band and hence contribute to interference. We also assume that every BS in each tier transmits with equal power. In the event that BSs in the same tier transmit with different power, we can further divide the tiers, known as thinning of the PPP. However, the result of this thinning is also a PPP. A specific example of a 3-tier BS network is shown in Figure 1. The location of the single antenna mobile is always assumed to be at the origin. Each BS is associated with two links, the direct link and the interfering link. The direct link is the link between the BS and mobile user, which is modeled as a Rician fading channel. In Rician fading, there is one significant path, also known as the LOS path, which has the maximum power, and multiple fading paths. The interfering links are modeled as Rayleigh fading channels, in which there are multiple signal paths, but none of them is dominant. These fading assumptions have previously been made in various analyses [9][10][11]. Also, we consider loss in power of the signal as it propagates in space, known as pathloss. This loss is due to dissipation of power transmitted by the BS, and the effects of the propagation channel.
All tiers will perform zero-forcing beamforming [6], which is a low-complexity detection method with assumed perfect CSI

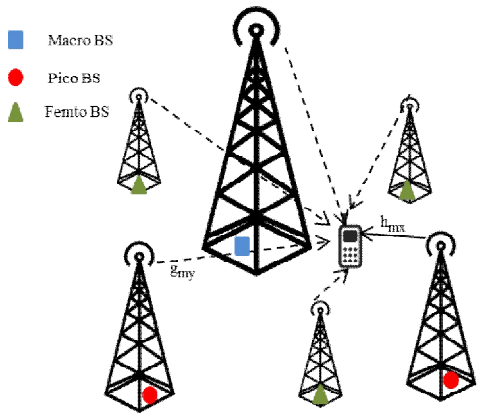

Figure 1: An illustration of a possible three-tier HetNet. The solid line indicates a direct link and the dashed lines indicate interfering links to the user

at the transmitter and the receiver. The probability of coverage is evaluated for multi user MIMO (MU-MIMO) multi-antenna technique. We also calculated the ASE which gives the number of bits transmitted per unit area per unit time per unit bandwidth.

2.2 BS Location Model

Consider the M-tier HetNet given by the set $\kappa = \{1,2,\dots M\}$ where each tier has BSs of a particular class, such as femto-cells, pico-cells or macro-cells, which are spatially distributed as independent PPP Φ_m with density $\lambda_m, \forall\, m \in \kappa$. Assume that the BSs in the m^{th} tier have power P_m with which they transmit to each user, deployment density λ_m, target signal-to-interference ratio (SIR) β_m, and number of transmit antenna $N_t^{(m)}$ [5].

2.2 Channel Model

The channel model is the main technical section of the paper. It is important to understand that the distribution of received power in the link between a typical multi-antenna BS and single-antenna mobile depends upon the multi-antenna technique employed, and whether or not the BS is acting as the signal provider to the user or as an interferer. In case the BS is acting as the provider to a typical mobile user, it precodes the signal based on the assigned transmission technique, which results in a different channel distribution in comparison to the scenario where it is acting as an interferer.
Each BS on the m^{th} tier is equipped with $N_t^{(m)}$ transmit antennas, while there are Ψ_m number of mobile users each having $N_r^{(m)}$ receiving antennas. In this case, we assume $N_r^{(m)} = 1$ i.e., one receiving antenna for each user. Let $\mathbf{z}_m = [z_{m1}\, z_{m2} \dots z_{mN_t^{(m)}}]^T$ denote the $N_t^{(m)} \times 1$ normalized signal vector transmitted by the BS providing link, and let $\mathbf{z}_j, j \in \kappa$ denote the interfering link. The received signal $\mathbf{y}_m$ from the m^{th} tier BS for a typical user located at the origin is given by

$$\mathbf{y}_m = \sqrt{P_m}\,\|x_0\|^{\frac{-\alpha}{2}}\,\mathbf{v}_{mx_0}^{*}\,\mathbf{z}_m + \sum_{j\epsilon\kappa}\sum_{y\epsilon\{\Phi_j\setminus x_0\}}\sqrt{P_m}\,\|y\|^{\frac{-\alpha}{2}}\,\mathbf{u}_{jy}^{*}\,\mathbf{z}_j \quad (1)$$

where P_m is the per user transmit power of the m^{th} tier BS [6]. The standard path loss function is given by $\|x_0\|^{\frac{-\alpha}{2}}$, where $\alpha > 2$ is the path loss exponent and $\|x_0\|$ is the distance between the mobile user and the serving BS. Here $\mathbf{v}_{mx_0}\epsilon\,\mathbb{C}^{N_t^{(m)}\times 1}$ is the direct link channel vector from the m^{th} tier BS located at x_0 to a typical user located at the origin and the interfering link vector from the j^{th} tier BS at y location is given by $\mathbf{u}_{jy}\epsilon\,\mathbb{C}^{N_t^{(m)}\times 1}$, and $*$ denotes the complex conjugate transpose.

The channel matrix $\mathbf{V}$ has two parts, a deterministic component $\mathbf{V}_d = \left(\mathbf{v}_{d,1}\mathbf{v}_{d,2}\ldots\mathbf{v}_{d,N_t^{(m)}}\right)$ associated with the LOS path, and a random component $\mathbf{V}_r = \left(\mathbf{v}_{r,1}\mathbf{v}_{r,2}\ldots\mathbf{v}_{r,N_t^{(m)}}\right)$ due to multipath fading components. For typical Rician fading, the channel matrix is written as

$$\mathbf{V} = \sqrt{\frac{K}{K+1}}\,\mathbf{V}_d + \frac{\sigma^2}{K+1}\,\mathbf{V}_r, \quad (2)$$

where it assumed for normalization [12] that $\|\mathbf{V}_d\|^2 = N_t^{(m)}\,N_r^{(m)}$ and $\mathbb{E}\{|\mathbf{V}_r|^2\} = 1$. Without loss of generality, we assume $\sigma = 1$. Note that, $K = 0$ corresponds to Rayleigh fading while $K \to \infty$ corresponds to non-fading channels. The columns of the channel matrix $\mathbf{V}$, denoted as $\mathbf{v}$, are assumed to be independent nonzero-mean complex circularly symmetric Gaussian column vectors distributed according to $\mathbb{CN} \in \left(\sqrt{\frac{K}{K+1}}\,\mathbf{v}_{d,i}, \frac{\sigma^2}{K+1}\,\mathbf{I}_{\Psi_m}\right)$ with $K \geq 0$ denoting the Rician factor, $\mathbf{v}_{d,i}$ for $i = 1\ldots\ldots N_t^{(m)}$ are a series of deterministic $\Psi_m \times 1$ columns vectors, independent across BSs and of the user distances [13].

Table 1: Notations Used in the Paper

Notation	Description
ϕ_m, λ_m	PPP describing the BS location in tier m; deployment density of PPP in tier m $\Phi = \cup_{m=1}^{M}\Phi_m$
P_m	BS transmit power in tier m
$N_t^{(m)}, \Psi_m$	No of transmit antennas at each BS in m^{th} tier; No of users in m^{th} tier
h_{mx}	Channel power of the direct link from a m^{th} tier BS located at x to a user
g_{my}	Channel power of the interfering link from a m^{th} tier BS located at y to a user

The elements of the column vector $\mathbf{u}$ are assumed to be independent and identically distributed (i.i.d) zero-mean, unit-variance, complex circularly symmetric Gaussian random variables, i.e. $\mathbb{CN}(0,1)$ [6]. We assume that the BSs have perfect knowledge of all channel matrices, and each mobile user has the perfect knowledge of its own channel matrix.

Assume that linear precoding is used in which the data symbol $\mathbf{s}_{m,i}$, from the m^{th} tier BS destined for the i^{th} user, for $1 \leq i \leq \Psi_m$ is multiplied by $\mathbf{w}_{m,i}$ so that the transmitted signal is a linear function, i.e. $\mathbf{z}_m = \sum_{i=1}^{\Psi_m}\mathbf{w}_{m,i}\mathbf{s}_{m,i}$. In linear precoding, zero-forcing (ZF) beamforming is one of the techniques used to serve users in all the tiers with perfect CSI at the BS.

The columns of the precoding channel matrix, $\mathbf{W}_m = [\mathbf{w}_{m,i}]_{1\leq i\leq\Psi_m}\,\epsilon\,N_t^{(m)} \times \Psi_m$, are found from the normalized columns of the channel matrix

$$\mathbf{W}_m = \widetilde{\mathbf{V}_m^{*}}\left(\widetilde{\mathbf{V}_m}\,\widetilde{\mathbf{V}_m^{*}}\right)^{-1}, \quad (3)$$

where $\widetilde{\mathbf{V}_m} = \left[\tilde{\mathbf{v}}_1,\ldots,\tilde{\mathbf{v}}_m\ldots\tilde{\mathbf{v}}_{\Psi_m}\right]^{*}\epsilon\,\Psi_m \times N_t^{(m)}$ is the concatenated matrix of channel directions, where the direction of each vector channel is represented as $\check{\mathbf{v}}_m = \frac{\mathbf{v}_m}{\|\mathbf{v}_m\|}$. The direct link channel power gain after precoding is given by,

$$h_{mx} = \left|\mathbf{v}_{mx}^{*}\mathbf{w}_{m,m}\right|^2 = \left|\widetilde{\mathbf{v}_m^{*}}\,\mathbf{w}_{m,m}\right|^2.\|\mathbf{v}_{mx}\|^2. \quad (4)$$

For users served via zero-forcing, the beamforming vectors, $\boldsymbol{w}$, are chosen such that $\boldsymbol{v}_{mx}^{*}\boldsymbol{w}_{m,i} = 0, \forall\, i \neq m, m \in \kappa$. In other words, it perfectly eliminates the signal contributions from all the other users.

In case of interfering links, the channel power gain is a sum of correlated random variables [14]. The correlation results from the fact that the precoding vectors are non-unitary in the zero forcing solution. Therefore, it is quite complex to compute the channel distribution, as the precoding vector $\mathbf{w}_j$ is calculated independently of $\mathbf{u}_{jy}$,i.e. the interference channel is independent of the channel used to compute $\mathbf{w}_j$. Hence, to avoid such problems, it is commonly assumed that for interfering links distribution, the precoding matrices have unit-norm orthogonal columns [14]. Therefore, $\tilde{\mathbf{u}}_{jy}$ and $\mathbf{w}_j$ are independent isotropic unit-norm random vectors, and $\left|\tilde{\mathbf{u}}_{jy}\mathbf{w}_j\right|^2$ is a sum of Ψ_j i.i.d exponential random variables. The distribution of interfering channel is approximated by the gamma distribution, $g_{jy} \sim \Gamma(\Psi_j, 1)$ [6].

Since we are interference limited, thermal noise is neglected in this work as it does not make any major variation in our results as demonstrated in [2][15]. The effects of thermal noise can be easily included if desired [9].

To calculate the signal-to-interference ratio, the received power at the typical mobile located at the origin from the BS located at $x_m \epsilon \phi_m$ is given by:

$$P_r = P_m h_{mx_m} \|x_0\|^{-\alpha}. \quad (5)$$

As we are neglecting the thermal noise, the received SIR can be expressed as

$$SIR(x_m) = \frac{P_m h_{mx_m} \|x_0\|^{-\alpha}}{\sum_{j\epsilon\kappa} \sum_{y\epsilon\{\Phi_j \setminus x_0\}} P_j g_{jy} \|y\|^{-\alpha}} \quad (6)$$

In order to associate cells with users, we assume that the set of the candidates serving BSs is the collection of the BSs that provide strongest instantaneous received power from each tier to which a mobile user is allowed to connect.

3. Coverage probability

According to the definition of coverage probability, a mobile user is said to be in coverage if its downlink SIR from at least one of the transmitting BSs is higher than the corresponding target SIR, β_m. Mathematically, it can be described as [5]

$$P_c = P\left(\bigcup_{m\epsilon\kappa} \max_{x_m \epsilon \Phi_j} SIR(x_m) > \beta_m\right), \quad (7)$$

where x_m is the location of the BS in the m^{th} tier and P is the probability that the maximum SIR in each tier calculated using (6) is greater than the target SIR denoted by β_m. We can also say that the coverage probability gives the average area in coverage or the average fraction of users served by the BSs using different multi-antenna techniques.

4. Area Spectral Efficiency

Another metric for quantifying system performance is Area Spectral Efficiency (ASE). It accounts for the fact that some techniques such as MU-MIMO serve a larger number of users than others, such as a Single user-beamforming (SUBF) system, which is a multiple-input single-output (MISO) multi-antenna technique that may result in a higher sum data rate [6].

ASE is defined as number of information bits transmitted per unit area per unit time per unit bandwidth,

$$\eta = \sum_{m\in\kappa} \Psi_m \lambda_m \log_2(1+\beta_m) P_c^{(m)}, \quad (8)$$

where $P_c^{(m)}$ is the per tier coverage probability, and β_m is the per tier target power. λ_m is the density of PPP (Φ_m), and Ψ_m is the number of users in each tier. For analytical comparison simplicity, we limit our comparison to $P_c^{(m)} = P_c$ for all tiers and require the same target SIR β_m for all tiers. ASE under this assumption is

$$\eta = P_c \log_2(1+\beta_m) \sum_{m\in\kappa} \Psi_m \lambda_m \quad (9)$$

We compare the ASE of MU-MIMO and the SISO case which are denoted as η_N and η_S, respectively. The ratio of ASEs can be expressed as

$$\frac{\eta_N}{\eta_S} = \frac{P_{c,N} \log_2(1+\beta_m) \sum_{m\in\kappa} \Psi_m \lambda_m}{P_{c,S} \log_2(1+\beta_j) \sum_{j\in\kappa} \Psi_j \lambda_j} \quad (10)$$

The ratio describes the gain in slope as the ASE is higher in MU-MIMO compared to the SISO case. Assume that the target SIR and the density are same for both MIMO and SISO cases, $\beta_m = \beta_j$ and $\lambda_m = \lambda_j$. The number of users in single-input single-output (SISO) case is one, i.e. $\Psi_j = 1$. Thus, (10) reduces to:

$$\frac{\eta_N}{\eta_S} = \frac{P_{c,N} \sum_{m\in\kappa} \Psi_m}{P_{c,S}} \quad (11)$$

which shows that the ratio of ASE grows with the number of users. In the next section, we will present simulation results which validate this observation that the ASE for MU-MIMO is higher than the SISO case for the system model assumed in this paper.

5. Numerical Results

In this section, we present the coverage probability and area spectral efficiency results obtained by running Monte Carlo simulations of the system model described in Section 4. These results are compared to those using a Rayleigh fading channel model.

Before we describe the actual results, we will briefly summarize the simulation procedure.

1) Choose a sufficiently large area where, for simplicity of simulation, a square area can be chosen with multiple tiers.
2) The location of BSs in different tiers can be simulated based on the realizations of independent PPPs of given densities.
3) Each base station has three quantities related to it: direct link parameter h_{mx}, interfering link parameter g_{my}, and the coordinates in the area chosen.
4) Assume that the mobile user lies at the origin. Calculate the channel parameters for the direct and interfering links, which are evaluated for a Rician fading channel and Rayleigh fading channels, respectively.
5) Calculate the received SIR from each BS. The mobile is in coverage if the received SIR from at least one of the BSs from any tier is larger than the corresponding target SIR.

Repeating the above mentioned procedure for a sufficient number of times gives an estimate of the coverage probability.

Using the methodology described above, we evaluate the coverage probability of the HetNet in the MU-MIMO case and obtain results for different values of Rician factor, K. We also compare the results of Rician fading with Rayleigh

Table 2: Coverage Probability in Rician Fading Parameters

Parameter	**Value**
Area	400
No of tiers, M	2
Power in each tier, P	[1,0.1]
Density of PPP λ_1, λ_2	[1,2]($\lambda_2 = 2\lambda_1$)
Pathloss exponent, α	3.8
Target SIR,β (in dB)	Varies from -8 to
Number of transmit antennas, $N_t^{(m)}$	2,3,4
Number of receiving antennas, $N_r^{(m)}$	1
No of users in each tier, Ψm	2,3,4
Rician factor, K	2

fading by setting the value of $K = 0$. Table 2 summarizes the simulation parameters for coverage probability evaluation.

5.1 Coverage Probability of Rician channel

Figure 2 is a plot that gives the probability of coverage, P_c, in Rician fading for the Rician factor, $K = 2$ evaluated for different values of target SIR, β_m. The number of antennas $N_t^{(m)}$ and users Ψ_m are assumed to be equal. Also, $N_t^{(m)}$ and Ψ_m are assumed to be same for both the tiers.

From Figure 2, it is clear that the coverage probability for 2 users and 2 transmitting antennas ($N_t^{(m)} = \Psi_m = 2$) is higher when compared to the case with 4 users and transmitting antennas $\left(N_t^{(m)} = \Psi_m = 4\right)$. This results from the fact that as the number of transmitting antennas and users increase, the inter-stream interference increases. Thus, the SIR denoted by

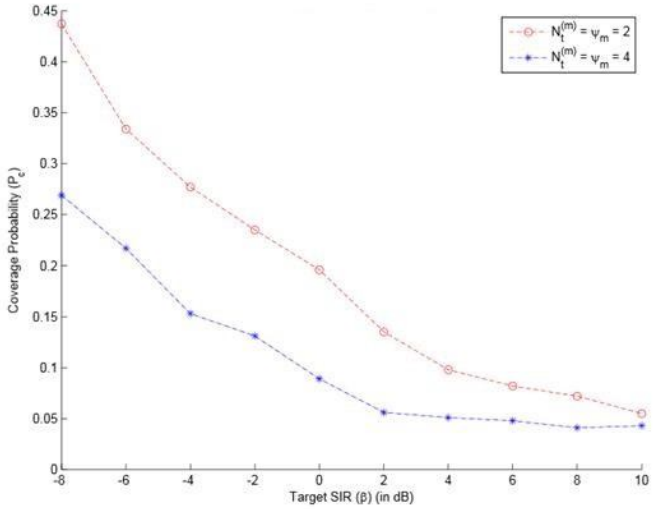

Figure 2: Probability of Coverage in Rician Fading for $K = 2$ for MU-MIMO

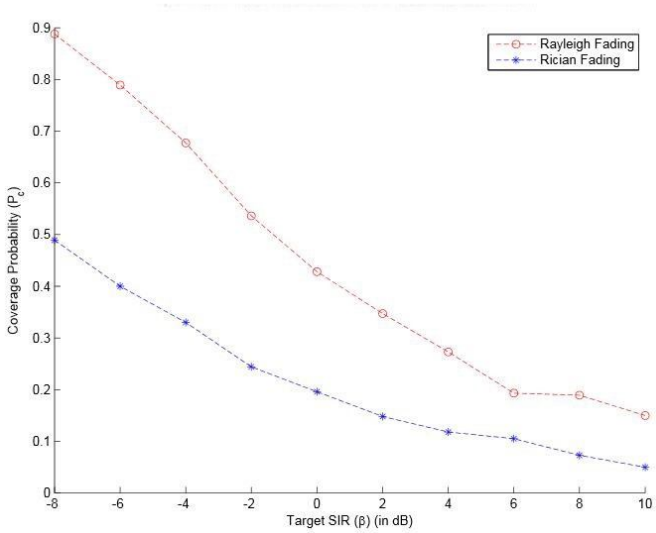

Figure 3: Comparison of coverage Probability in Rayleigh and Rician fading for $K = 1$

(7) reduces, and in turn coverage probability decreases for all cases of users and transmitting antennas.

5.2 Comparison of coverage probability of Rician with Rayleigh channel

Having discussed the coverage probability results for Rician fading with 2 and 4 users/transmitting antennas cases we present Figure 3 that shows the comparison of coverage probability in Rayleigh and Rician Fading. The number of transmit antennas and users is chosen to be 2 for this evaluation. The Rician fading is evaluated for $K = 1$, while Rayleigh fading is the case when $K = 0$, i.e. there is no line of sight between the transmitter and receiver.

We observe that the coverage probability in Rician fading is lower than in Rayleigh fading, since an increase in K emphasizes on the deterministic part of the channel, which leads to an increase in the correlation coefficient. A high correlation coefficient limits the number of independent paths carrying information. Hence, the coverage probability in Rician fading is lower than Rayleigh fading.

Rician fading should perform the same as Rayleigh fading when the fading factor is zero [16]. In order to validate our results and ensure that the simulation results for the Rician fading model "collapses" back to Rayleigh fading, we change the value of $K = 1$ to $K = 0$. The result in Figure 4 confirms the fact that the Rician fading ($K = 0, N_t^{(m)} = \Psi_m = 2 \; or \; 4$) closely follows the Rayleigh fading $N_t^{(m)} = \Psi_m = 2 \; or \; 4$).

The Rayleigh fading curves on Figure 4 were obtained by replicating the model suggested in [7] with the channel power distribution of both the direct and interfering links following a Gamma distribution.

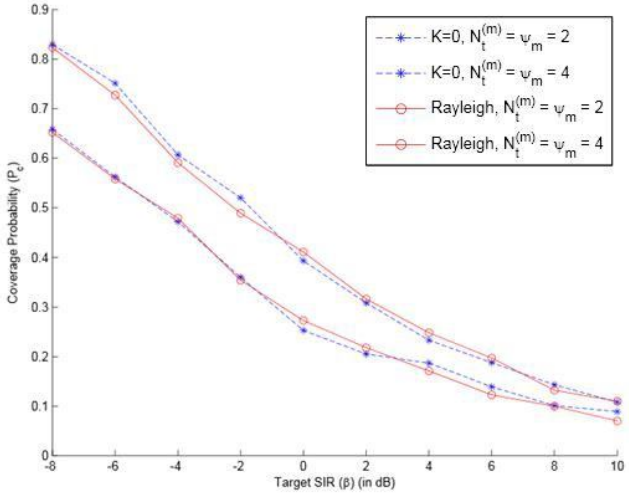

Figure 4: Comparison of coverage Probability in Rayleigh and Rician fading for $K = 0$

5.3 Area Spectral Efficiency

According to equation (11), the ratio of ASEs is the ratio of the product of coverage probability and the sum of all the users in each tier in MU-MIMO, to the coverage probability in SISO case. The probability of coverage in MU-MIMO case is evaluated for varying values of $N_t^{(m)}$ which is equal to Ψ_m. The value of Rician factor, K is chosen to be 1. Figure 5 shows that the ASE in MU-MIMO case is always higher than in SISO as the ASE ratio is mostly greater than 1. The ASE of MU-MIMO increases with an increase in the number of transmitting antennas $N_t^{(m)}$ as is evident from Figure 5.

Figure 6 represents the ratio of ASEs of MU-MIMO and SISO calculated over increasing values of K. The number of transmitting antennas and users in this case is 4. As we observe from the Figure 6, the ASE ratio decreases with increase in value of K. This is accounted by the fact that an

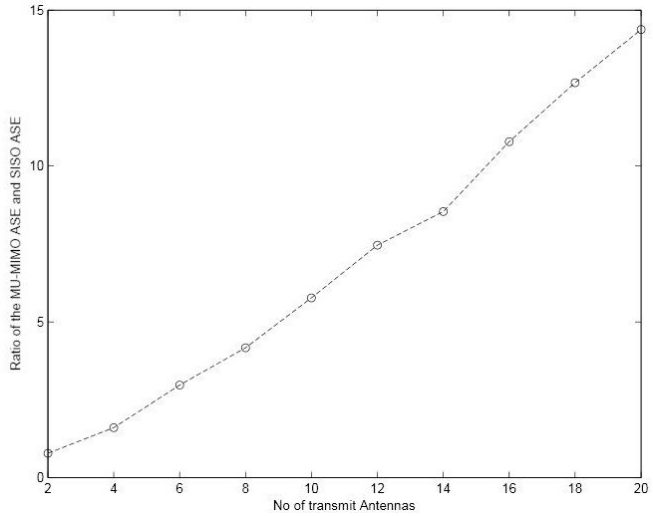

Figure 5: Ratio of Area Spectral efficiency in Rician fading

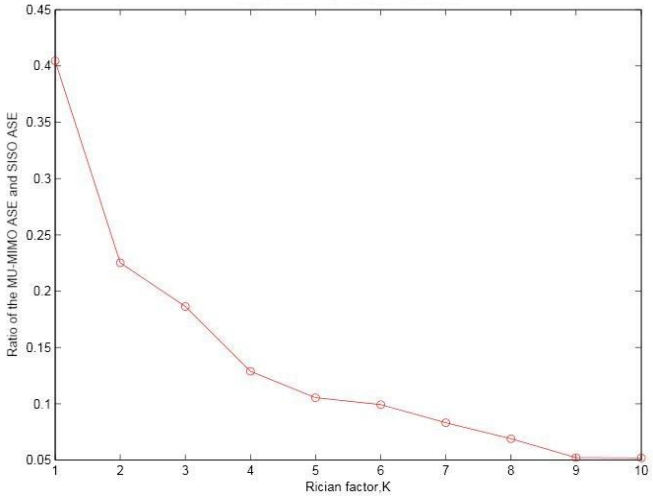

Figure 6: Ratio of Area Spectral Efficiency with varying K

increase in K results in a decrease in coverage probability due to an increase in the correlation coefficient. A high correlation coefficient restricts the number of independent paths carrying information, resulting in lower coverage probability.

6. Conclusion and Future Work

Through simulation and analytical study, we have obtained the coverage probability in a multi-tier, multi-antenna HetNet with Rician fading. As expected in channel fading, the probability of coverage decreases with increase in number of transmit antennas and users, due to the increase in inter-stream interference. The comparison of coverage probability in Rician fading with Rayleigh fading reveals that the MU-MIMO system provides a higher probability of coverage to a mobile when it is not in the line-of-sight, i.e. in case of Rayleigh fading. This is due to the fact that Rician fading limits the number of independent paths to the mobile user.

The ASE simulation results reveal that MU-MIMO can support a larger number of users with an increase in transmit antennas. Also, the ASE decreases with the increase in the Rician factor, K, when the number of transmit antennas are fixed. Thus, we conclude that MU-MIMO leads to a lower coverage probability but higher ASE as compared to a single antenna system for the same deployment density.

For future work, we plan to obtain a closed form distribution of channel coefficients in Rician fading channel with MU-MIMO. A general extension to this work would be closed form expressions for the coverage probability as well as ASE in Rician fading environment. Also, these performance metrics could be studied in different fading environments such as Nakagami fading, and for different precoding techniques such as MMSE, which were not investigated here. The possibility of evaluating the coverage probability and ASE without the restrictions of using the same number of users and transmit antennas could also be explored.

REFERENCES

1. D. Gesbert, M. Shafi, D. Shiu, P. J. Smith, and A. Naguib, "**From theory to practice: An overview of mimo space-time coded wireless systems**," *IEEE Journal on Selected Areas in Communications*, vol. 21, no. 3, pp. 281–302, Sep. 2006.
2. J. G. Andrews, F. Baccelli, and R. K. Ganti, "**A Tractable Approach to Coverage and Rate in Cellular Networks**," *IEEE Transactions on Communications*, vol. 59, no. 11, pp. 3122–3134, 2010.
3. R. K. Ganti, "**A Tractable Approach to Coverage and Rate in Cellular Networks**," Ph.D. dissertation, Univ. of Notre Dame, Indiana, December 2009.
4. H. S. Dhillon, R. K. Ganti, F. Baccelli, and J. G. Andrews, "**Modeling and Analysis of K-tier Downlink Heterogeneous Cellular Networks**," *IEEE Journal on Selected Areas in Communications*, vol. 30, no. 3, pp. 550–560, 2012.
5. H. S. Dhillon, M. Kountouris, and J. G. Andrews, "**Downlink coverage probability in MIMO HetNets**," in *Conference Record of the Forty Sixth Asilomar Conference on Signals, Systems and Computers*, 2012, pp. 683–687.
6. H. S. Dhillon, M. Kountouris, and J. G. Andrews, "**Downlink MIMO HetNets: Modeling, Ordering Results and Performance Analysis**," *IEEE Transactions on Wireless Communications*, vol. 12, no. 10, pp. 5208– 5222, 2013.
7. J. Hoydis, A. Kammoun, J. Najim, and M. Debbah, "**Outage perfor- mance of cooperative small-cell systems under Rician fading channels**," in *Int. Workshop Signal Processing Advances in Wireless Communications*(SPAWC'11), 2011, pp. 551–555.
8. Z. Jak and G. Jeney, "**Coverage analysis for macro users in two-tier Rician faded LTE/small-cell networks**," *Wireless Networks*, pp. 1–10, 2015.
9. R. H. Y. Louie, M. R. McKay, and I. B. Collings, "**New performance results for multiuser optimum combining in the presence of Rician fading**," *IEEE Transactions on Communications*, vol. 57, no. 8, pp. 2348–2358, 2009.
10. M. R. McKay, A. Zanella, I. B. Collings, and M. Chiani, "**Error probability and SINR analysis of optimum combining in Rician fading**," *IEEE Transactions on Communications*, vol. 57, no. 3, pp. 676–687, 2009.
11. C. Chayawan and V. A. Aalo, "**On the outage probability of optimum combining and maximal ratio combining schemes in an interference- limited Rice fading channel**," *IEEE Transactions on Communications*, vol. 50, no. 4, pp. 532–535, 2002.
12. C. Siriteanu, S. D. Blostein, A. Takemura, H. Shin, S. Yousefi, and S. Kuriki, "**Exact MIMO Zero-Forcing Detection Analysis for Transmit- Correlated Rician Fading**," *IEEE Transactions on Wireless Communica-tions*, vol. 13, no. 3, pp. 1514–1527, 2014.
13. A. Maaref and S. A¨ıssa, "**Capacity of MIMO Rician fading channels with transmitter and receiver channel state information**," *IEEE Transactions on Wireless Communications*, vol. 7, no. 5-1, pp. 1687–1698, 2008.
14. R. W. H. Jr., T. Wu, Y. H. Kwon, and A. C. K. Soong, "**Multiuser MIMO in Distributed Antenna Systems With Out-of-Cell Interference**," *IEEE Transactions on Signal Processing*, vol. 59, no. 10, pp. 4885–4899, 2011.
15. V. K. Garg, **Wireless Network Evolution: 2G to 3G**. Prentice Hall, 2001.
16. A. Goldsmith, **Wireless Communications**. Cambridge University Press, 2005.